Stony Brook University

The Antimicrobial Properties of Zinc-Releasing Bioceramics

A Thesis Presented

by

Xin He

to

The Graduate School

in Partial Fulfillment of the

Requirements

for the Degree of

Master of Science

in

Materials Science and Engineering

Stony Brook University

May 2012

Stony Brook University

The Graduate School

Xin He

We, the thesis committee for the above candidate for the

Master of Science degree, hereby recommend

acceptance of this thesis.

Yizhi Meng – Thesis Advisor
Assistant Professor, Materials Science and Engineering

Dilip Gersappe – Second Reader
Associate Professor, Materials Science and Engineering

Michael Hadjiargyrou – Third Reader
Associate Professor, Biomedical Engineering

This thesis is accepted by the Graduate School

Charles Taber
Interim Dean of the Graduate School

Abstract of the Thesis

The Antimicrobial Properties of Zinc-Releasing Bioceramics

by

Xin He

Master Degree

in

Materials Science and Engineering

Stony Brook University

2012

Up to 80% of nosocomial infections are caused by biofilm-producing bacteria such as Staphylococci and Pseudomonas aeruginosa. These types of microorganisms can become resistant to antibiotics and are difficult to eliminate. As such, there is tremendous interest in developing bioactive implant materials that can help to minimize these post-operative infections. Using water-based chemistry, we developed an economical, biodegradable and biocompatible orthopedic implant material consisting of zinc- doped hydroxyapatite (HA), which mimics the main inorganic component of the bone. Because the crystallinity of HA is typically too compact for efficient drug release, we substituted calcium ions in HA with zinc during the synthesis step to perturb the crystal structure. An added benefit is that zinc itself is a microelement of the human body with anti-

inflammatory property, and we hypothesized that Zn-doped HA is an inherently antibacterial material. All HA samples were synthesized by a co-precipitation method using aqueous solutions of Zinc nitrate, Calcium Nitrate, and Ammonium Phosphate. XRD data showed that Zn was successfully incorporated into the HA. The effectiveness of Zn-doped HA against a model biofilm-forming bacterium is currently being evaluated using a wild-type strain and a streptomycin- resistant strain of *Pseudomonas syringae* pv. *papulans* (Psp) which is a plant pathogen isolated from diseased apples.

Key words: Hydroxyapatite, Zinc, Citrate, Pseudomonas, Antibacterial.

Table of content

List of tables

List of Figures

Acknowledgement

I would express my deep and most sincere gratitude to my advisor, Professor Yizhi Meng, for her continuous guidance on scientific research and help with my graduate study. I learned a lot from her, not only the academic, she is the most energetic and enthusiastic professor I have ever met. Her passion towards the knowledge and research will inspire me in my future life.

I would thank my committee members, Prof. Dilip Gersape, and Prof. Michael Hadjiargyrou, for their guidance of my experiments and advice of my thesis.

Besides, I would like to thank all my lab members who helped me, advised me, studied with me, worked with me, and the most important: had the most wonderful time with me. They are Kathryn Dorst, Xia Lu, Chi Zhang, Gaojun Liu, Cheng Zhang, Ling Li, Amanda Chin, Junyi Wu, Derek Rammelkamp, Kai Song and Giulia Suarato.

Also thanks to Xia Zhao, Shelagh Zegers, Zofia Baumann, researchers in Stony Brook University and Dmytro Nykypanchuk, Xiao-Liang Wang, Vesna Stanic and Weiqiang Han, the scientists from Brookhaven National Lab, for their help to my experiments.

Last but not the least, I must thank my parents Ping He and Jingmei He, who supported my graduate study and gave their endless love to me. I couldn't finish my study without their encouragement and support. Thank you.

Introduction

Up to 80% of nosocomial infections are caused by biofilm-producing bacteria, such as *Staphylococci* and *Pseudomonas aeruginosa* [1]. These types of microorganisms can become resistant to antibiotics and are difficult to eliminate. As such, there is tremendous interest in developing bioactive implant materials that can help to minimize these post-operative infections.

On the other hand, controlled release technology is one of the advancing scientific areas of bioengineering and human health care [2]. Drug release has become one of the important issues during the past decades. Scientists always wanted to find some green materials can carry the drug inside and release it as close to the zero order. The word "green" means not only the product itself is green, nontoxic, and good compatible but also the raw materials are no harmful to the environment or human body as well as the whole synthesis process.

Inorganic materials have some advantages over the polymeric materials because its low toxicity and simple structure opposite to the polymeric ones. Among the inorganic materials, hydroxyapatite (HA), as a carrier of drug, protein and antibiotics, has attracted much attention of its good bioactivity and biocompatibility [3]. But the most important reason people choose this material, as the drug carrier is that HA is the main composition of the bone. It is a totally green material even during the synthesis period, there would be no harmful chemicals formed.

However, HA has a perfect and compact structure of crystallinity and also a limited surface area and unpredictable bioresorbability, thus makes HA is typically too

compact for efficient drug release. To change the crystallinity, we substituted calcium ions in HA with zinc during the synthesis step to perturb and modify the crystal structure of the material. Zinc itself is an essential trace element in human body and it has the antibacterial effect. Also, citrate salt was added to increase the dispensability of the hydroxyapatite and bounded with calcium and zinc to form a better material, which itself has antibacterial effect.

1 Literature review

1.1 Medical Microbiology

Microbiological issues have always been in the public view. The antibiotic-resistant bacteria, the food poisoning, the HIV, bird flu, etc. are all that matters that have drawn lots of attention [4, 5]. The microorganism or microbe has a large group of members that are extremely diverse, which organisms group that are lumped together on the same basis of one property. Generally, they are so small that they can only be seen with the use of a microscope. Viruses, bacteria, fungi, protozoa and some algae are all members of this group [6].

1.1.1 Nosocomial infections

Wound infection is one of the most important issue in nosocomial care management [7]. Two million cases of nosocomial infections occur in the Unites States annually and more than half are caused by the indwelling devices. Especially problematic are the infections acquired after implant surgery [8]. It is estimated that 80% of the nosocomial infections are caused by biofilm-forming microorganisms [9]. Bacteria attached on the surface of the wound aggregate by the weak Van der Waals force, then the adhered bacteria rapidly proliferate, recruit other cells then produce a sticky material containing bacteria called biofilm [10]. The figure 1. shows the schematic cycle of this process.

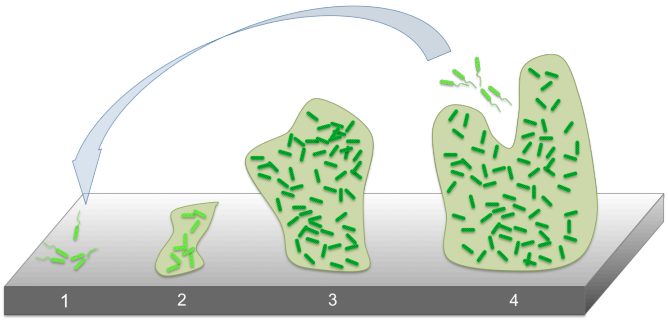

Fig. 1 The schematic representation of biofilm development and progression. (1) Individual free-floating bacteria populate on the surface. **(2)** Attachment becomes irreversible and extracellular polymeric substance is produced. **(3)** The structure of biofilm develops and becomes mature. **(4)** Detachment and dispersion of individual bacterium to repeat the cycle. [10]

Among the infections, Gram-negative *Pseudomonas aeruginosa (P. aeruginosa)* and Gram-positive *Staphylococcus aureus (S. aureus)* are two of the most common-forming bacteria [11]. The *P. aeruginosa*, is resistant to many antibiotics [12].

1.1.2 *Pseudomonas*

Pseudomonads have a widespread occurrence bacterium in nature. They appeared early in the microbiology history and were classified by the end of the 19th century [13]. The genus *Pseudomonas* has a diverse group of family. It is a Gram-negative bacterium, aerobic non-sporulating rod that can move by means of polar flagella, thus not allowing a clear distinction from other Gram-negative bacterial groups. It is an environmentally and biologically important bacterium that can biodegrade manmade toxic chemicals and join the plant-bacteria interaction [12, 14, 15].

Pseudomonas syringae is a rod-shape, plant pathogen that can infect a wide range of plant species, and exists as over 50 different strains. The individual cell of *Pseudomonas syringae* exists within different microbial communities on large numbers of leaves like lilac leaves and tomato plant leaves on almost all kinds of the terrestrial plant species [16]. *Pseudomonas syringae* is responsible for the surface frost damage in frost sensitive plants such as herbs, fruits and vegetables [17]. According to ABSA (American Biological Safety Association), *Pseudomonas syringae* is categorized as Risk Group Level 2 and classified as only the plant pathogen but not human or animal pathogen.

Pseudomonas syringae pv. *papulans* (*Psp*) is the bacterium that can cause apple or pear to affect severely of blister spot, and more commonly apples of the cultivar Mutsu [18, 19]. It is a serious disease characterized by dark brown blisters on fruits, tiny cankers on branches and distortion of leaves [20].

1.1.3 Antibiotics and bacteria

The Gram staining tests simply divide bacteria into two types: Gram-positive and Gram-negative. The differences between the two types are chemical and physical properties of their cell walls. Generally, it detects peptidoglycan, which is present in a thick layer in Gram-positive bacteria. A Gram-positive test results in a purple/blue color while a Gram-negative will result in a pink/red color.

The most practical use of the Gram staining test is, usually, Gram-positive bacteria are sensitive to penicillin, however, none of the Gram-negative bacteria is, they are more afraid of streptomycin, etc. This is very important in clinical care: if an infection

occurs causing by bacteria, we have to know which kind of bacteria it is, then we can choose the right antibiotics to kill the bacteria.

There are many limitations of the antibiotics use in clinical. Almost all strains of *S. aureus* in the United States are now resistant to penicillin, with many also resistant to newer methicillin related drugs (e.g. MRSA: Methicillin-Resistant *Staphylococcus aureus*) [10]. The MRSA is also called Multidrug-RSA or Oxacillin-RSA and such strains are also frequently resistant to most of the widely used antimicrobial agents, including the aminoglycosides, macrolides, chloramphenicol, tetracycline, and fluoroquinolones, etc. [21]. The MRSA is troublesome for patients recovering hospital and can weaken their immune system, leading to a greater risk of infections by other microorganisms [22].

1.2 Controlled drug release

Controlled release of the drug has great advantages compared to the traditional drug release system: low toxicity, high efficacy and improved patient compliance. The aims of all controlled release systems are trying to enhance the effectiveness of the drug [2].

Generally, controlled drug release refers to delivery drug that extends a specific duration during the treatment. In contrast to the conventional injection of the medicine every period of time, the drug concentration of the controlled release will remain a stable and controllable domain [23]. Some reviews reported using microspheres for drug delivery. In ***Vasir*** *et al.*'s review paper [24], they summarized using a bioadhesive polymeric microsphere for a controlled drug delivery. In ***Müller*** *et al.*'s paper [25], the authors presented the production of by making the nanosuspension that make the drug

into nanoparticles on a laboratory scale. In ***Freiberg*** *et al.*'s review paper [26], they summarized the common polymer microspheres for controlled drug release.

1.3 Bone composition

The majority of the bone is made of bone matrix [27]. Generally bone tissue is composed by ~30wt% protein-based collagen reinforced by a ~70wt% nanosized dispersed mineral phased hydroxyapatite crystals which give the hardness and rigidity to the bone [28]. Also in the enamel: the hardest part of the human body, it contains ~97wt% of hydroxyapatite [29].

1.3.1 Hydroxyapatite

Apatite, a compound family that has similar hexagonal crystal structure, is the main component of the biological hard tissue [30]. Hydroxyapatite is a natural mineral with the chemical formula of $Ca_5(PO_4)_3OH$, which consist most of the inorganic part of the bone. HA crystal is hexagonal in structure and in each unit cell contains tow entities [28, 29, 31].

HA is now being used as cell scaffolds to enhance bone regenerations in healing of orthopedic and tooth loss in dental surgery. In addition, attributed to its chemical composition, when used in tissue engineering, it can provide calcium and phosphate that are essential elements for the bone.

1.3.2 Zinc

Zinc is an essential trace element for animals ranging from 0.0120 to 0.0250 wt% in human bone, much higher than it in the fat free adult tissue and plasma, which contains 0.0030 Zn wt% and 0.78-1.0 mg/L [32]. Zinc also plays an important role in taste perception, the patient with hypogeusia (decreased taste acuity) exhibit lower zinc concentration in serum [33].

As a component of orthopedic implant coatings, zinc could also promote bone formation around the implant, which could shorten the recovery time. However, supplemental zinc must be controlled by a slow release rate because zinc at a high level may cause adverse reactions. Too much zinc could inhibit the absorption of other vitamins and minerals [32]. Also a negative correlation between excessive zinc and sperm count as well as sperm motility was found in the experiments of mice [34].

1.3.3 Doped HA

In the last 20 years, doped HA have been starting used for controlled drug delivery. ***Dasgupta*** *et al.* used Zn and Mg doped HA to test the release properties of protein [3]. ***Palazzo*** *et al.* investigated the adsorption and desorption of the anticancer drug *cis*-diamminedichloroplatinum (II) (CDDP, cisplatin) and the new platinum (II) complex di(ethylenediamineplatinum)medronate (DPM) with HA-drug nanocrystals [35]. The radius of zinc atom is 1.22 Å and the radius of calcium atom is 1.76 Å while both the Zn^{2+} and Ca^{2+} ions are divalent. The substitutions of calcium with zinc atoms would not change the whole structure type but may cause some imperfection in the crystal

potentially increasing the release efficiency compared to the pure HA [3]. In some reports the results that Zn-doped HA showed a better release rate than the pure HA [36]. HA doped with other metal ions such as strontium, magnesium, etc. have shown to promote osteoblast functions and subsequent bone formation [3, 37, 38]. Additionally, studies have indicated zinc deficiency in elderly subjects may cause osteoporosis [39]. Therefore, zinc doped HA has the potential to provide good biocompatibility and excellent osteogenic properties [40].

1.4 Citrate salt

Citrate [$C_3H_5O(COO)_3^{3-}$] (Fig. 2), naturally exists in citric acid and citric salt and is produced in several chemical forms. Citric acid, sodium citrate and potassium citrate are the most commonly form and widely used in food additive field, especially sodium citrate, is used in carbonated beverages, fruit drinks, jams, jellies, gelatin desserts, cheese and dairy products, etc. [41].

Small organic compounds like citrates are widely found in the biological tissues [42]. The citrate in bone is many times higher than the other body tissue [43]. NMR has shown that the bound citrate accounts for 5.5 wt% of the organic composition in bone and covers apatite at a density of about 1 molecule per 4 nm^2. In the bone it is not loosely dissolved but strongly bound mainly because the interaction of [COO^-] group and Ca^{2+}, with its three carboxylate groups at distances of 3 to 4.5 Å from the apatite surface [44].

Citrate is both non-planar and contains three carboxylic groups, making it an excellent model for studying the role of the acidic peptides and proteins that are considered to be important modulators of biomineralization [45].

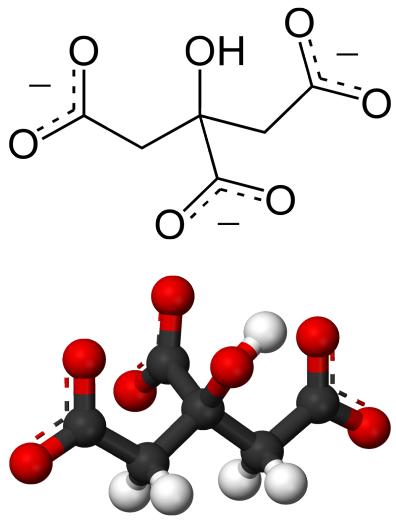

Fig. 2 The structure of the citrate group

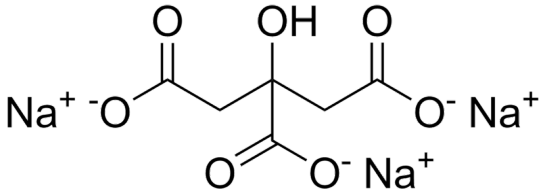

Fig. 3 The structure of trisodium citrate

In ***Sreenivasan*** *et al*.'s study, using the zinc citrate formulation revealed lower rates of intra-oral microbial biofilm formation. Results from HA squares placed in the patients' oral stents demonstrate similar inhibitions of the anaerobic bacteria and *streptococci* after the use of zinc citrate for 5 hours indicating its effectiveness in reducing biofilm formation [46].

Objective

Therefore the objective of this thesis was to test these following hypotheses:

1) Zinc doping of HA can enhance the release rate by perturbing the crystalline structure in a dose-dependent manner.
2) Addition of citrate to zinc doped HA can increase the dispersibility of zinc and may have antimicrobial effects against biofilm-forming bacteria.
3) Doping of HA with zinc and addition of citrate may have additive effects and can enhance the antimicrobial properties of drug such as streptomycin.

2 Materials and Methods

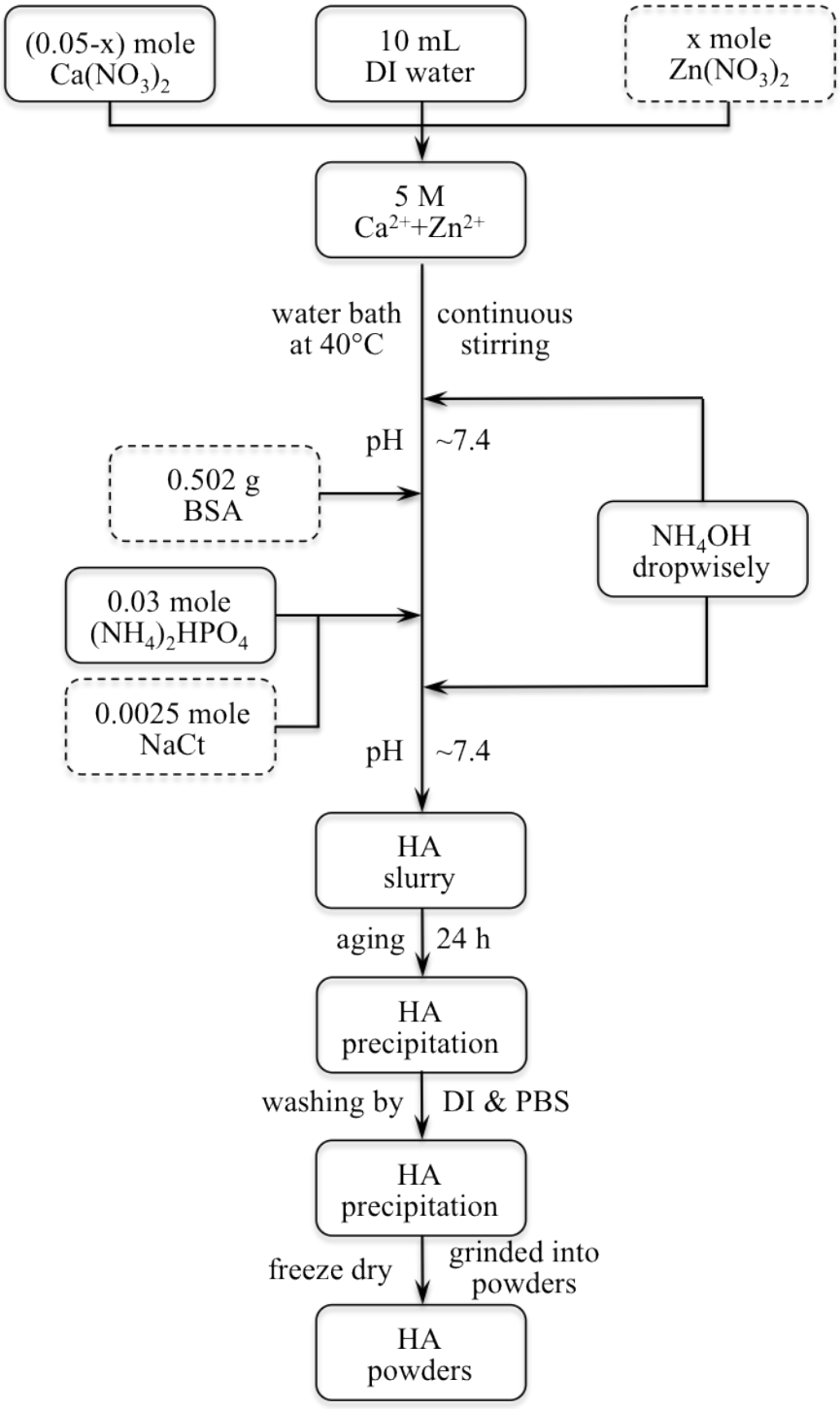

Fig. 4 The flow charts of the synthesis of Zn doped/undoped HA with/without BSA and sodium citrate. (**x** was chosen from 0, 0.0005, 0.0025, 0.005)

2.1 Synthesis of the hydroxyapatite

Hydroxyapatite can be written as the chemical as $Ca_5(PO_4)_3OH$. The well-known, wet chemical precipitation method [3, 47-52] was used as the procedure of the hydroxyapatite synthesis and lyophilization method was used to dry the materials.

The chemical reaction equation is:

$$\mathbf{5Ca(NO_3)_2 + 3(NH_4)_2HPO_4 + 4(NH_4)OH \rightarrow Ca_5(PO_4)_3OH + 10NH_4NO_3 + 3H_2O}$$

Calcium nitrate tetrahydrate ($Ca(NO_3)_2 \cdot 4H_2O$, 99+%, for analysis ACS) was purchased from Acros Organics. Zinc nitrate hexahydrate ($Zn(NO_3)_2 \cdot 6H_2O$, 98%, reagent grade) and ammonium phosphate dibasic ($(NH_4)_2HPO_4$, ≥98%, ACS reagent) were purchased from Sigma-Aldrich Chemical Co. (St. Louis, MO, USA).

2.1.1 Hydroxyapatite

Briefly, 5 M Ca^{2+} solution was made by dissolving 0.05 mole calcium nitrate tetrahydrate in to 10 mL deionized water (DI) and stirred at 40°C in water bath. Then ammonium hydroxide ($(NH_4)OH$ or $NH_3 \cdot H_2O$) was added to bring the pH value around 7~7.4. After that, 0.03 M ammonium phosphate dibasic was added into the solution. After continuous stirring and maintaining the pH around 7.2~7.4 for 30 minutes, the solution changed into a slurry. The slurries were conserved in clean 50 mL tubes and aged for 24 hours at room temperature. After aging, the slurry was centrifuged at 2500 rpm for 10 minutes. Supernatant was collected and phosphate buffer saline (PBS) and DI

were used to wash the precipitation. Then the precipitates were centrifuged again and supernatant was decanted. The obtained precipitations were frozen at -80°C overnight and freeze-dried before being ground into powder form.

2.1.2 Zinc doped hydroxyapatite

Three different zinc substitutions were selected: 1%, 5%, 10% molar ratio.

Zinc doped hydroxyapatite were synthesized by combining different amount molar ratios of calcium nitrate (1%, 5% and 10%) with zinc nitrate, prior to dissolving in DI. The quantities of the reagent were maintained to provide a (Ca+Zn)/P = 1.67/1 molar ratio.

Table 2-1 Composition of zinc-doped hydroxyapatite (molar ratio)

	HA	1%Zn-HA	5%Zn-HA	10%Zn-HA
$Ca(NO_3)_2$	0.05	0.0495	0.0475	0.0450
$Zn(NO_3)_2$	0	0.0005	0.0025	0.0050
$(NH_4)_2HPO_4$	0.03	0.03	0.03	0.03

The chemical reaction equation is (x=1%, 5%, 10%, respectively):

$$\mathbf{5(1-x)\ Ca(NO_3)_2 + 5x\ Zn(NO_3)_2 + 3\ (NH_4)_2HPO_4 + 4\ (NH_4)OH \rightarrow}$$

$$\mathbf{Ca_{5(1-x)}Zn_{5x}(PO_4)_3OH + 10\ NH_4NO_3 + 3\ H_2O}$$

2.2 Drug loading and the addition of the citrate

First, Bovine Serum Albumin (BSA) (OmniPur®, Fraction V heat shock isolation), purchased from EMD Chemicals Inc., was used as the model drug. Then, streptomycin sulfate salt ($C_{21}H_{39}N_7O_{12} \cdot 1.5H_2SO_4$, BioReagent, suitable for cell culture, powder, MW 728.69), purchased from Sigma-Aldrich Chemical Co., was used to test the antibacterial effect of the material.

2.2.1 BSA loading

During the synthesis of hydroxyapatite or zinc doped HA, 10wt% of Bovine Serum Albumin (BSA) was added after combining the calcium and zinc nitrate. When the powder was fully dissolved into the solution, ammonium phosphate was then added into the solution. The pH of the entire process was maintained around 7~7.4 and the temperature was maintained at 40°C.

2.2.2 Citrate loaded hydroxyapatite

The sodium citrate was added with the ammonium phosphate. A nominal (Ca+Zn) to citrate molar ratio of 20:1 was used [53].

Sodium citrate (tribasic dihydrate, $Na_3C_6H_5O_7 \cdot 2H_2O$, ≥99%, molecular biology, MW 294.1) purchased from Sigma-Aldrich Chemical Co., was added during the synthesis of the hydroxyapatite.

2.3 Characterization of the materials

2.3.1 BSA release test

To test the release kinetics of BSA, 10mg of BSA-loaded and unloaded hydroxyapatite was added into 10 mL of PBS in the 15 mL Falcon® tubes (BLUE MAX™ Jr. 15 mL Polystyrene Conical Tube, 17×120mm style, sterile). Then the tubes were placed on a rocking platform (Incubating Rocker, Incubating 3-D Rotating Waver, VWR™ International) at room temperature with a 15 degrees tilt. At each time point (every 24 hours) 1 mL liquid samples were transferred to 1.7 mL microcentrifuge tubes (Costar®, 1.7 mL prelubricated, natural, graduated, non sterile, non pyrogenic, RNase/DNase free) and put into -20°C freezer, followed by centrifuging for 5 minutes at 2500 rpm. 1 mL PBS was then added into each tube to maintain the total volume at 10 mL.

BSA release was tested for 7 days. Then the Bicinchoninic Acid Assay (BCA assay) was used to test the concentration of the protein in each sample. For calibration, the 0, 0.5 μg/mL, 5 μg/mL, 10 μg/mL, 20 μg/mL, 40 μg/mL standard BSA in PBS solutions were also tested with the BCA assay, to draw the linear regression curve. Each sample was calibrated by its non-BSA incorporated HA sample.

2.3.2 Thermo gravity analysis (TGA)

PerkinElmer Diamond TG/DTA was used in TGA. 5 mm aluminum open sample pan was used to test. The heat started from 50.00 °C to 550.00 °C at the rate of 20.00

°C/min. Then the sample temperature was held at 550.00 °C for 15 minutes and then cooled down from 550.00 °C to 50.00 °C at the rate of 70.00 °C/min.

2.3.3 X-ray diffractometry (XRD)

Both synchrotron beamline X-ray diffraction test and benchtop X-ray diffraction were carried out at Brookhaven National Laboratory, Upton, NY.

For synchrotron XRD, the wavelength of the X-ray was 0.65255Å, and energy was 6.5-19keV (focused). The source type was bending magnet, and the optical system was monochromator: Si (111) channel-cut located 10 m from source. Samples were placed in air 100 mm from the detector screen.

For benchtop XRD, X-ray wavelength was 1.54056Å (Cu). The scanning angle started from 20.000° to 50.000°, sample weight was about 0.01g, the scanning speed was 2.00°/s, X-ray energy was 80kV, by the Rigaku MiniFlex™ II, Desktop X-ray Diffractometer. The samples were placed on greased plastic plate and metal.

2.3.4 Fourier transform infrared spectroscopy analysis

Dry powders were used for Fourier transform infrared spectroscopy (FTIR), pure sodium citrate and BSA were also tested as a control. The images were acquired by Thermo SCIENTIFIC Nicolet 6700 FT-IR.

Measurements in air were used as background, ethanol and propanol were used to clean the substrate of the samples in between measurements.

2.4 Antibacterial activity assays

Pseudomonas syringae pv. *papulans (Psp)* (kindly donated by Professor Thomas Burr) were used as the bacteria in the experiment. Two strains were used. *Psp-32* Mutsu apple fruit lesion from Wayne Co., NY that is the strain sensitive to streptomycin. *Psp-37* Mutsu apple fruit lesion from Sodus, NY that is a strain resistant to streptomycin.

2.4.1 Bacterial cell culture

Pseudomonas agar F plates were used to grow the bacteria. Basically, 5 mL glycerol (Glycerin 1,2,3-Propanetriol, $C_3H_8O_3$, ≥99%, molecular biology) purchased from Sigma-Aldrich Chemical Co., and 17.5g *Pseudomonas* agar (HIMEDIA® M120, for fluorescein) purchased from VWR™ International, was dissolved into distilled water to make a 500 mL solution in a glass bottle. Then the solution was autoclaved 15 minutes at 121°C then slowly exhausted. After the solution cooled down a little bit, it was poured into 25 plates (Fisherbrand® Sterile 100 mm×15 mm polystyrene petri dish). After the plates cooled down to the room temperature, they were sealed them with parafilm® and stored them in the 4 °C fridge.

When culturing the bacteria, 1 loop of the bacteria gel was transferred to the agar F plate. Then the plates were kept at room temperature for 48 hours until visible bacteria colonies were formed.

Growth curve of *Pseudomonas syringae* pv. *Papulans* was tested "terrific broth" [54]. Generally, 6g Tryptone (Microbiologically tested, Sigma-Aldrich), 12g yeast extract (BioReagent, plant cell culture tested, Sigma-Aldrich), 2 mL glycerol were dissolved in distilled water to make a 450 mL solution in a 500 mL glass bottle with continuous

stirring. Then the solution was autoclaved 15 minutes at 121°C then slowly exhausted. 1.16g potassium phosphate monobasic (KH_2PO_4, ≥99.0%, cell culture tested, Sigma-Aldrich) and 6.275g potassium phosphate dibasic (K_2HPO_4, ≥99%, molecular biology, Sigma-Aldrich) were dissolved in 50 mL sterile distilled water. After the autoclaved solution cooled down to the room temperature, the potassium phosphate solution were poured into the glass bottle, and then the volume of the solution was adjusted by sterile distilled water to 500 mL.

To get the growth rate curve, 3 full loops of the *Psp* that was cultured on the plate for 48 hours was dissolved in the 20 mL terrific broth in a 50 mL Falcon tube and then vortexed to disperse the bacteria. At each time point, 0.8 mL media was extracted and mixed with 0.8 mL 70% glycerol into a 1.7 mL tube. Then the mixture was stored in the -20°C freezer immediately. After 5 days, the optical density of all the samples were tested at 600 nm using BIO – RAD SmartSpec™ 3000 in Biomedical Engineering in Stony Brook University. Pure terrific broth with glycerol was used as a blank control.

2.4.2 Logarithm reduction test

For the logarithm reduction test, terrific broth was used as the media. Depending on how much media was needed, several loops of bacteria grown on the plates were transferred into the media.

Generally, all glassware were autoclaved to make sure it is sterile, then *Psp* was cultured in the terrific broth. The ratio of the bacteria of the media was 3 loops per 100 mL terrific broth. After the bacteria dispersed well in the media, they were allowed to grow for 1 hour. Then OD600 was tested with the pure sterile terrific broth as the

background. When the OD600 value reached 0.1, bacteria were transferred to media to different beakers containing different doped/undoped HA samples in media. One beaker was pure bacteria media, grown in Terrific Broth as the positive control.

2.4.3 Zone of inhibition

Hydroxyapatite powders were first pressed into pellets. The pellets were placed in the 20 mL glass bottle (20 mL disposable scintillation vial), and autoclaved 20 minutes and dried 15 minutes at 134°C.

1 loop of *Psp* cultured on the plate for 48 hours was dissolved in 5 mL the terrific broth in 15 mL Falcon tube and vortexed to make it a well-dispersed solution. The solution was diluted until its OD600 value was 0.1 (pure terrific broth was used as the blank). Then 1 mL solution was put on one agar F plate and bacterial cell spreader (25mm, Clenceware®) was used to spread the bacteria solution on the surface of the agar.

Triplicates of each citrate loaded/unloaded pure HA, 1%Zn-HA, 5%Zn-HA, 10%Zn-HA pellets were put on one plate with the *Psp* coating. One plate with no pellets and only the coating was also placed as the positive control. The plates were incubated at room temperature for 3 days, to see if there would be a clear zone of bacteria inhibition around the pellets.

3 Results

3.1 XRD

Figure 5 showed the synchrotron XRD data of BSA loaded/unloaded hydroxyapatite synthesis in neutral (pH 7) and basic (pH 9) conditions.

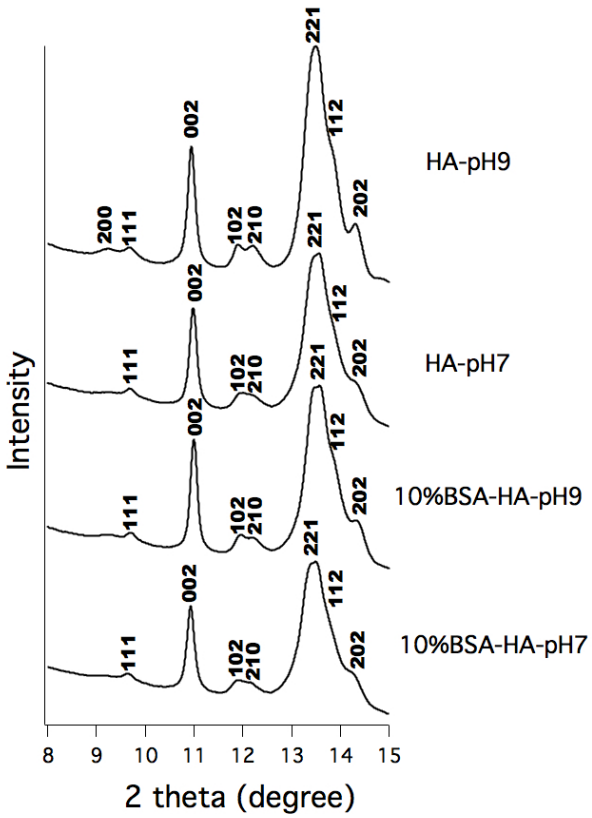

Fig. 5 The X-ray diffraction spectra of (a) HA-pH9: the HA synthesized at pH9**; (b)** HA-pH9: the HA synthesized at pH7.4**; (c)** 10%BSA-HA-pH9: the 10%BSA loaded HA synthesized at pH9**; (d)** 10%BSA-HA-pH9: the 10%BSA loaded HA synthesized at pH7.4, **by synchrotron with X-ray wavelength of 0.65255Å**

All the samples showed two characteristic synchrotron XRD peaks around 2-theta value of 10.9° and 13.3°, which indicated the 002 and 211 phases [55], respectively, of

pure hydroxyapatite. The BSA unloaded HA formed in basic condition showed the strongest intensity. BSA loaded HA and HA formed in neutral condition showed weaker intensity and broadening peaks, and the peaks merge could also be seen.

Fig. 6&7 showed the benchtop XRD data of Zn doped/undoped hydroxyapatite samples XRD data.

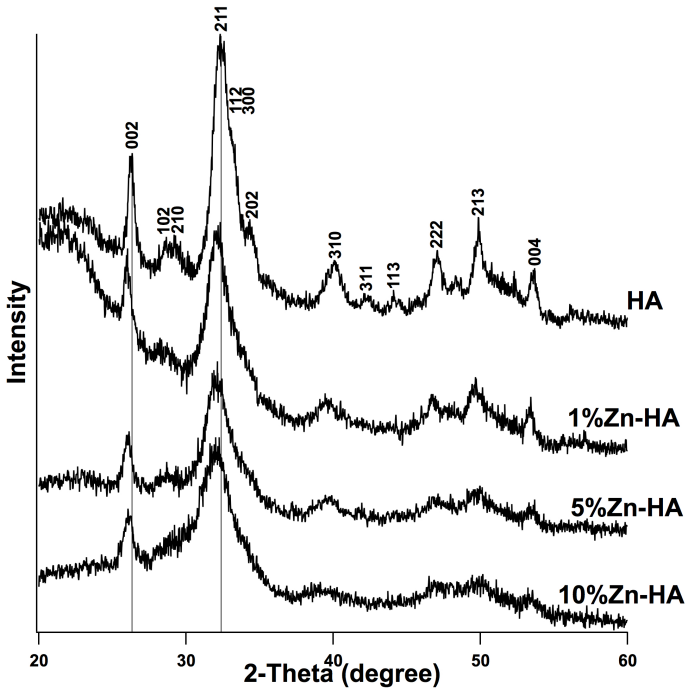

Fig. 6 The X-ray diffraction figures of (a) HA: pure hydroxyapatite**; (b)** 1%Zn-HA: 1% Zn doped HA**; (c)** 5%Zn-HA: 5% Zn doped HA**; (d)** 10%Zn-HA: 10%Zn doped HA, **by Desktop X-ray Diffractometer which the wavelength is 1.54056Å**

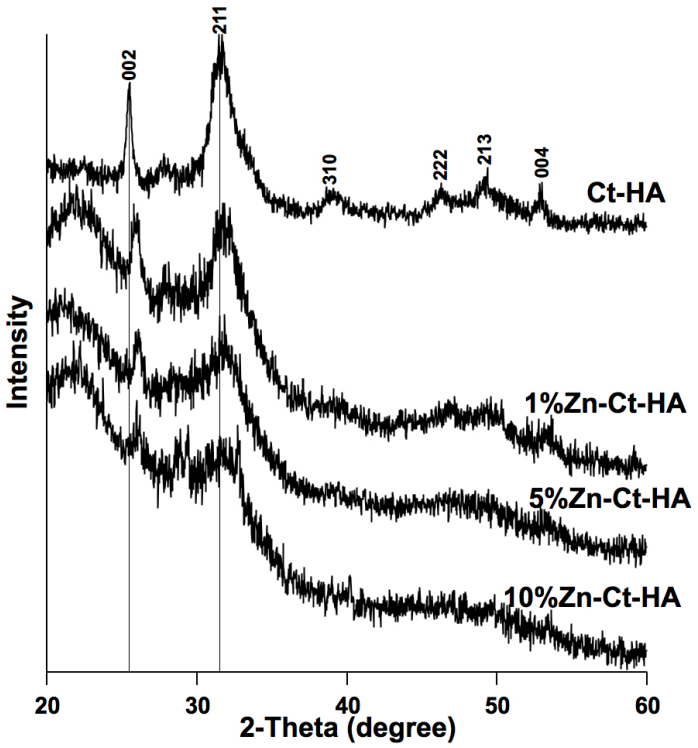

Fig. 7 The X-ray diffraction figures of (a) Ct-HA: pure hydroxyapatite with citrate**; (b)** 1%Zn-Ct-HA: 1% Zn doped HA with citrate**; (c)** 5%Zn-Ct-HA: 5% Zn doped HA with citrate**; (d)** 10%Zn-Ct-HA: 10%Zn doped HA with citrate, **by Desktop X-ray Diffractometer which the wavelength is 1.54056Å**

All the samples showed two characteristic benchtop XRD peaks around 2-theta values of 26° and 32°, which indicated the 002 and 211, respectively, of pure hydroxyapatite. All Zn-doped samples showed lower intensity and broadening peak compared to non-doped samples. The 211 peak of 10%Zn-HA was significantly weaker than the pure HA sample, as were the 002, 310, 222, 213 peaks (Fig. 6). Peak 002 appeared merged into peak 211 in the 10%Zn-HA sample, and the peak 211 is much broader than the pure HA sample, which meant a lower crystallinity.

Also from the Fig. 6&7, the 2-theta indicate 211 and 002 peaks shifted. Below is the table calculating the ***d***-spacing of the 211 and 002 planes for different samples.

Table 3-1 The *d-spacing* of non-citrate Zn-doped/undoped HA. (Å)

	HA	1%Zn-HA	5%Zn-HA	10%Zn-HA
002	3.3808	3.3985	3.4088	3.4165
211	2.7676	2.7693	2.7844	2.7928

Table 3-2 The *d-spacing* of citrate added Zn-doped/undoped HA. (Å)

	HA	1%Zn-HA	5%Zn-HA	10%Zn-HA
002	3.5037	3.4529	3.4398	3.4269
211	2.8466	2.8203	2.8082	2.7347

The data from the table 3-2, the non-citrate HA shows increasing the zinc concentration increased the ***d***-spacing of the 002 HA from 3.3808 Å to 3.4165 Å, and 211 HA from 2.7676 Å to 2.7928 Å, respectively.

From the table 3-3, the citrate added HA shows increasing the zinc concentration decreased the ***d***-spacing of the 002 HA from 3.5037 Å to 3.4269 Å, and 211 HA from 2.8466 Å to 2.7347 Å, respectively.

3.2 Fourier transform infrared spectroscopy analysis

Compared with pure Zn doped/undoped HA sample, both citrate added and BSA-loaded samples showed extra peaks.

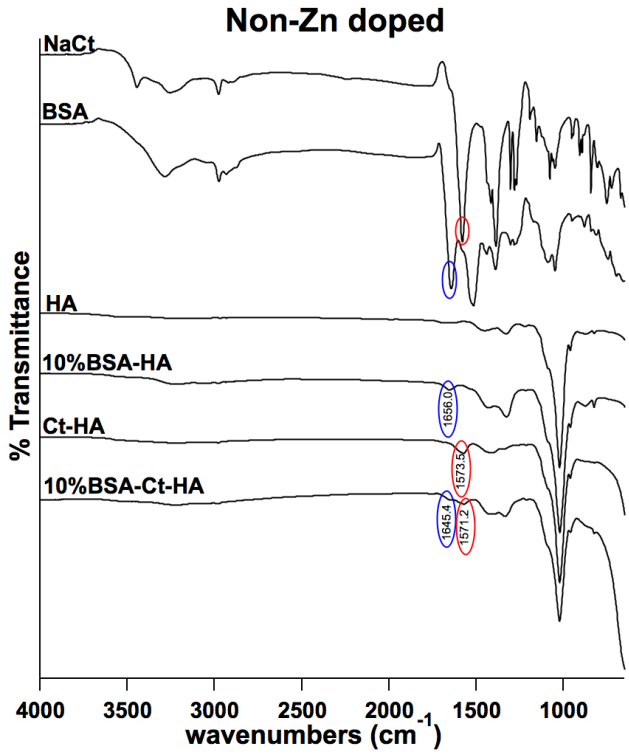

Fig. 8 FTIR spectra of non-Zn doped HA: (a)NaCt: sodium citrate; **(b)BSA:** BSA protein; **(c) HA:** pure hydroxyapatite; **(d)10%BSA-HA:** 10%BSA incorporated HA; **(e)Ct-HA:** citrate added HA; **(f)10%BSA-Ct-HA:** 10%BSA incorporated, citrate added HA. Wavenumber from 4000 cm^{-1} to 650 cm^{-1}.

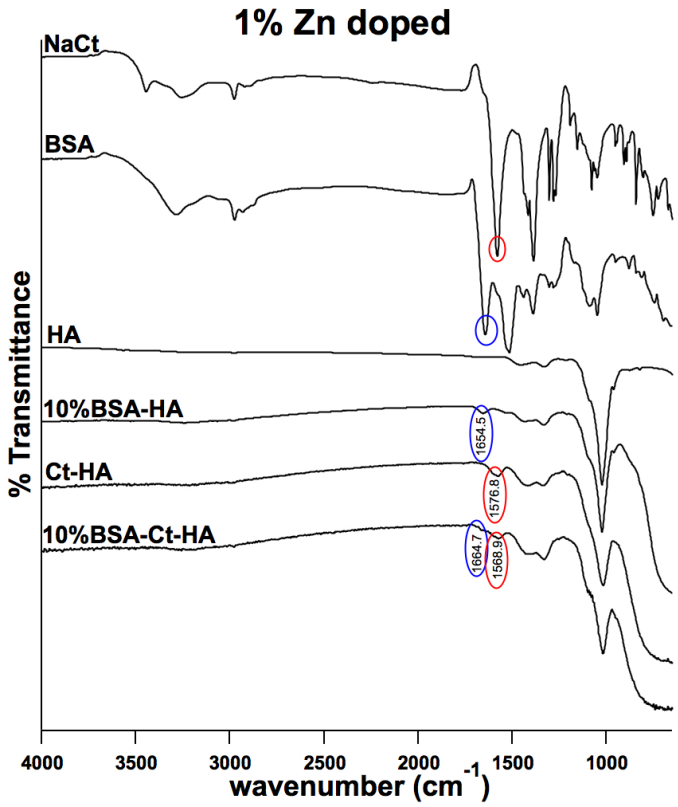

Fig. 9 FTIR spectra of 1%Zn doped HA: (a)NaCt: sodium citrate; **(b)BSA:** BSA protein; **(c) HA:** 1%Zn doped hydroxyapatite; **(d)10%BSA-HA:** 10%BSA incorporated 1%Zn-HA; **(e)Ct-HA:** citrate added 1%Zn-HA; **(f)10%BSA-Ct-HA:** 10%BSA incorporated, citrate added 1%Zn-HA. Wavenumber from 4000 cm^{-1} to 650 cm^{-1}.

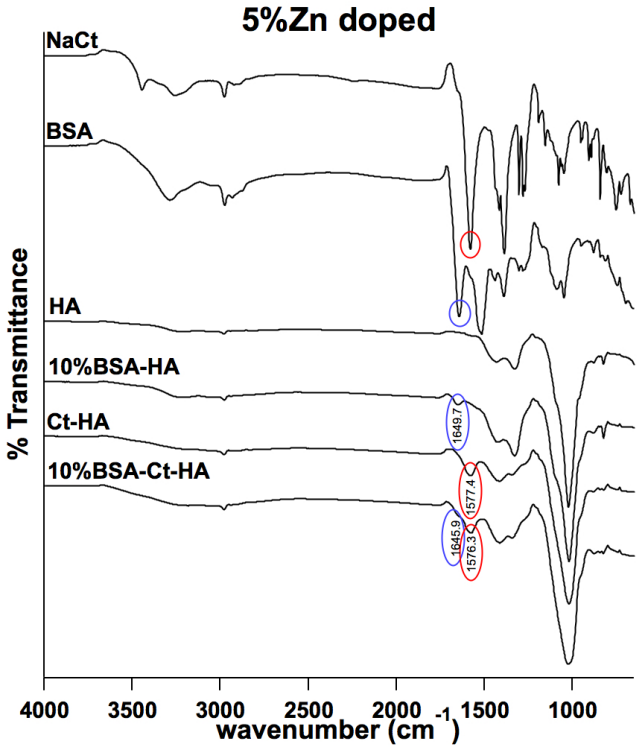

Fig. 10 FTIR spectra of 5%Zn doped HA: (a)NaCt: sodium citrate; **(b)BSA:** BSA protein; **(c) HA:** 5%Zn doped hydroxyapatite; **(d)10%BSA-HA:** 10%BSA incorporated 5%Zn-HA; **(e)Ct-HA:** citrate added 5%Zn-HA; **(f)10%BSA-Ct-HA:** 10%BSA incorporated, citrate added 5%Zn-HA. Wavenumber from 4000 cm^{-1} to 650 cm^{-1}.

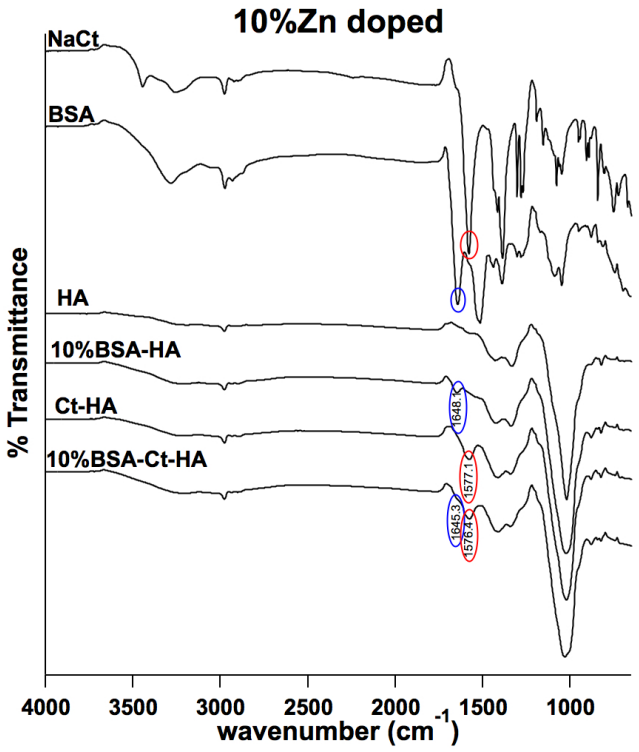

Fig. 11 FTIR spectra of 10%Zn doped HA: (a)NaCt: sodium citrate; **(b)BSA:** BSA protein; **(c) HA:** 10%Zn doped hydroxyapatite; **(d)10%BSA-HA:** 10%BSA incorporated 10%Zn-HA; **(e)Ct-HA:** citrate added 10%Zn-HA; **(f)10%BSA-Ct-HA:** 10%BSA incorporated, citrate added 10%Zn-HA. Wavenumber from 4000 cm^{-1} to 650 cm^{-1}.

The blue circles showed the peaks from BSA around 1650 cm^{-1}, and the red circles showed the peaks from citrate around 1580 cm^{-1}.

3.3 Growth rate of the *Pseudomonas syringae* pv. *papulans*

The growth rate of the *Psp* is shown in the Fig. 12, the time point was selected for 0, 12, 16, 20, 24 hours for every 24 hours.

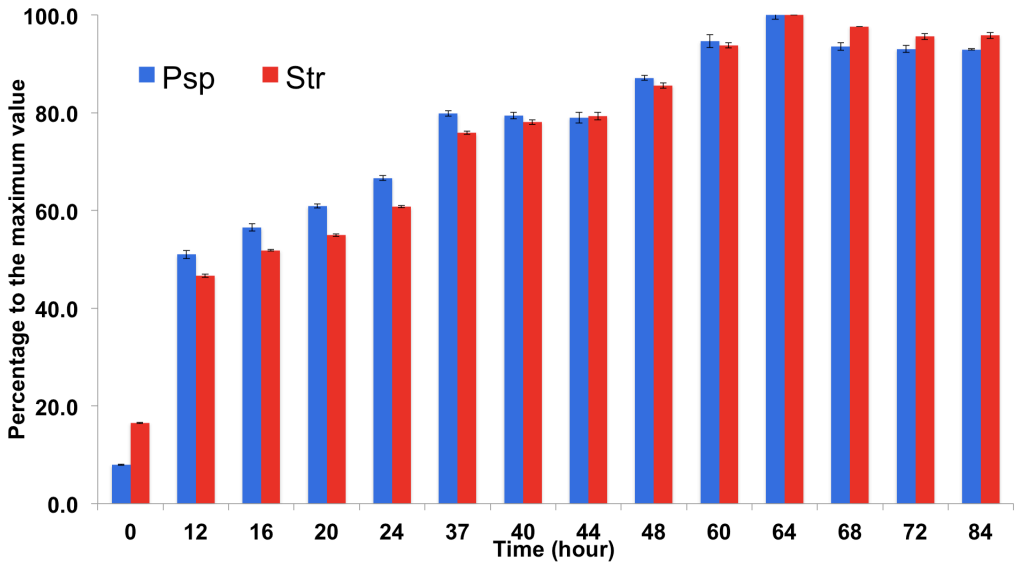

Fig. 12 The growth rate curve of *Pseudomonas syringae* pv. *Papulans* (*Psp*: *Psp*-32; *Str*: *Psp*-37)

The peak in growth rate for both strains was at 64 hours. That means the death rate of both bacteria became faster than the growth rate around 64 hours, and after that time point, cell numbers maintain a relatively stable period indicating that the bacteria did not proliferate after 64 hours.

3.4 Zone of inhibition

Below are the pictures of the different samples tested in Zone of Inhibition (ZoI). There were inhibition zones around the both non-citrate and citrate added pellets of HA, 1%Zn-HA, 5%Zn-HA, 10%Zn-HA samples. This means the antibacterial effect was shown in all these samples in 2 days.

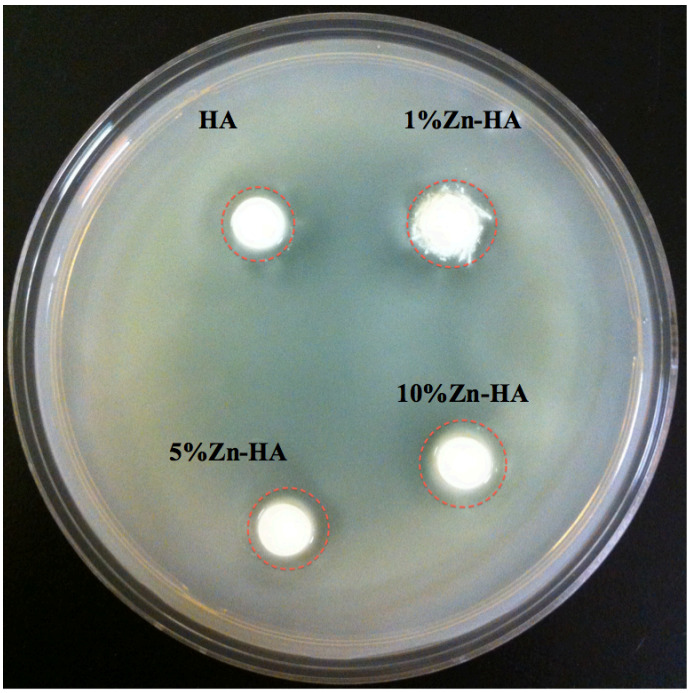

Fig. 13 The zone of inhibition test, HA, 1%Zn-HA, 5%Zn-HA, 10%Zn-HA without citrate pellets incubated on a culture of *Pseudomonas syringae* pv. *Papulans.* Photos were taken after 2 days of culture.

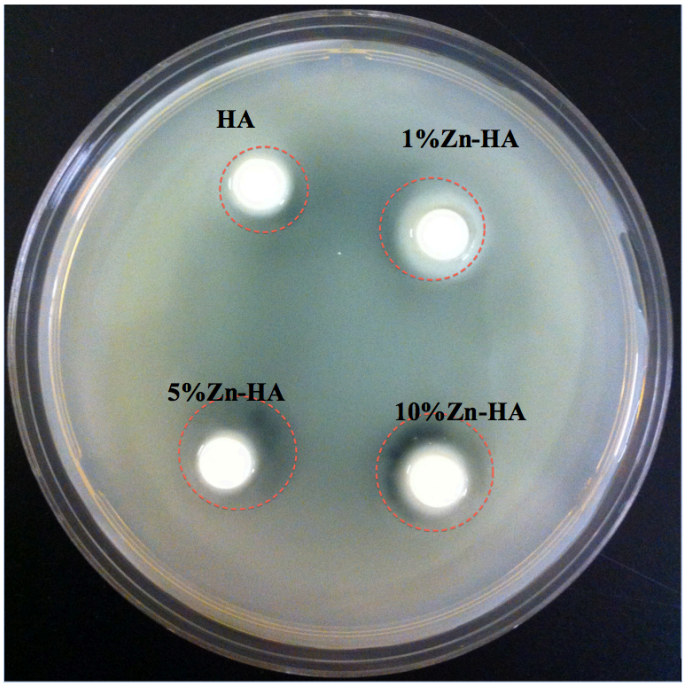

Fig. 14 The zone of inhibition test, HA, 1%Zn-HA, 5%Zn-HA, 10%Zn-HA with citrate added pellets incubated on a culture of *Pseudomonas syringae* pv. *Papulans.* Photos were taken after 2 days of culture.

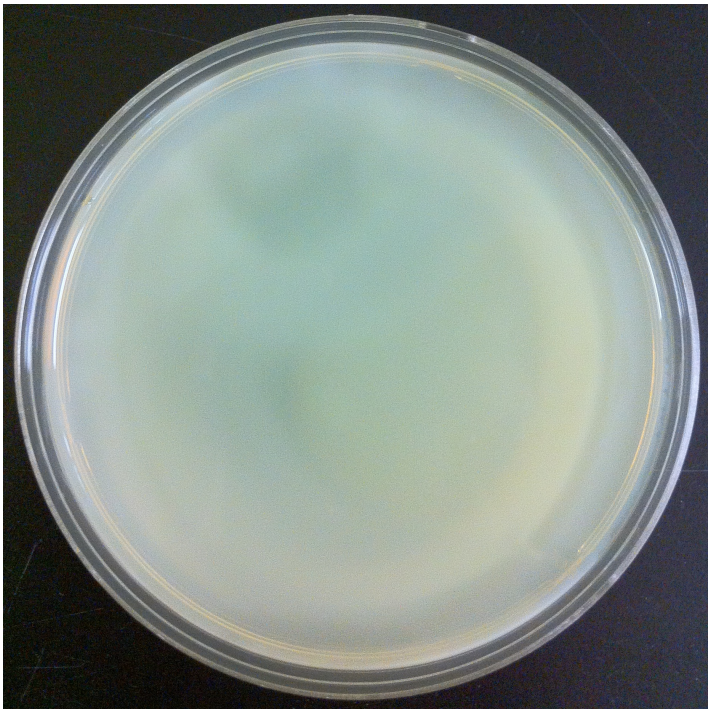

Fig. 15 The bacteria grown on the agar plate only. Photos were taken after 2 days of culture.

The red circles were drawn to show the zone of inhibition. The diameters of the ZoI were measured and shown in table 3-4. (The diameter of the pellet was 8 mm.)

Table 3-3 The diameter of the Zone of Inhibition of different samples after bacteria grown 2 days. (mm)

Samples	Zone of Inhibition	
	Non-citrate	Citrate added
HA	11.0±0.5	12.0±1.0
1%Zn-HA	12.5±0.5	15.0±3.0
5%Zn-HA	12.5±0.5	17.0±4.0
10%Zn-HA	13.0±1.0	18.0±2.0

The zone of inhibition test showed higher Zn concentration increased the diameter of ZoI. Also, with the addition of citrate, the diameter of ZoI were larger than non-citrate samples.

4 Discussion

From the BSA release results and XRD data, it is apparent that release from the Zn doped samples was faster compared to the undoped HA. The XRD data showed the Zn doped samples had lower crystallinity suggesting that Zn doping may have perturbed the hydroxyapatite's strong hexagonal structure, which may have accelerated the release of BSA.

From the XRD data, we calculated the ***d***-spacing of both 211 and 002 planes of all the samples. From the table 3-2, ***d***-spacing of both 211 and 002 planes increased with the increasing of the Zn concentration. It proved that Zinc doping of HA could perturb the crystalline structure in a dose-dependent manner. Compared with non-citrate samples, citrate added samples in general had a larger ***d***-spacing of both 211 and 002 planes. The only exception was the 211 phase of the 10%Zn-doped citrate-HA, which had a slightly smaller d-spacing than all other samples (Table 3-3). This may be caused by the highly amorphous structure. From the XRD spectra figure 7, the 10%Zn spectrum was very amorphous. Both the 211 and 002 peaks were very weak. Also this may have been due to experimental error and needs to be repeated. This showed that with the addition of citrate, the crystallinity could be further decreased by the coordination between the Ca^{2+} and citrate group.

The FTIR test showed both the BSA and citrate salt were loaded successfully into the (Zn-) HA. The peaks around 1650 cm^{-1} of BSA come from the α-helix (1658-1651 cm^{-1}), β-sheet (1640-1610 cm^{-1}), turn (1670-1665 cm^{-1}) and random coil (1648-1641 cm^{-1}) [56]. The peaks around 1575 cm^{-1} of the citrate come from the amide II (N-H bending).

We set the initial concentration of *Psp* in the broth for 3 loops/20 mL during the growth rate experiments. Different initial concentration of bacteria in the broth would lead to different growth rate: lower initial concentrations would slow down the growth rate and higher initial concentrations would accelerate the growth. If we set the initial concentration the same, the time of bacteria to reach the maximum concentration would be the same, which in our experiment was 68 hours.

Bacteria proliferated better in the liquid media as nutrients diffuse faster than on the plates. Also bacteria cultured on the plates could not float around to acquire nutrient and oxygen. So it is reasonable that *Psp* grew more slowly on the agar F plates than in the terrific broth.

We set the initial concentration of ZoI test as 0.5-loop/20 mL, which was much lower than the bacteria growth rate experiment. However, to assure the *Psp* were in a healthy growing condition, all bacteria were harvested after 48 hours of growth for the microbiology experiments for both culture on the plates and Zone of Inhibition test.

During the Zone of Inhibition test, the non-citrate added group showed mild antibacterial effect. The diameter of ZoI increased slightly from 11.0 mm to 13.0 mm. This indicated Zn can help boost the antibacterial effect. With the addition of citrate, the diameter increased further from 12.0 mm to 18.0 mm. This shows that with the citrate, the antibacterial effect increased dramatically. Among these samples, the non-citrate undoped HA showed the least antibacterial effect, and the 10%Zn doped, citrate added HA showed the largest diameter of ZoI.

We also tested the relation between the antibacterial effects of Zn-HA and the volume of broth put on the plate in the ZoI experiments. At first we put 1 mL broth with

the bacteria grown homogeneously with the initial concentration of 0.5-loop/20 mL, none of the non-citrate samples showed any antibacterial effect, while the citrate added group showed mild antibacterial effect by a smaller diameter of ZoI. Then we increased the volume of broth spread on the plates to 2 mL, and then it showed a much better result. Both the non-citrate and citrate added group showed that the inhibition zone and the diameters of the ZoI of citrate added samples were larger. By carefully observing the plates, 1 mL of broth was too little for a plate to grow and the Zn is hard to diffuse out since the plate became very dry after 24 hours, and the color of the plate become darker than with 2 mL broth on the plates.

5 Conclusion

In this study, we successfully synthesized the hydroxyapatite by using the wet chemical condition. From the XRD spectra, different zinc concentrations changed the ***d***-spacing of the 221 and 002 planes of the hydroxyapatite, which indicated zinc was loaded successfully. The FTIR showed extra peaks of BSA or/and citrate incorporated samples, which indicated BSA and citrate were incorporated successfully.

After that, *Pseudomonas syringae* pv. *Papulans* was cultured in the "terrific broth" to test the growth rate. Around 68 hours the bacteria reached the highest concentration. Considering the bacteria was cultured in the media with high concentrated nutrition, the bacteria grown on the agar plates would have a lower growing speed. However, in order to make sure the bacteria were still alive and very active, we harvested the bacteria around 48 hours immediately preceding the Zone of Inhibition test. From the ZoI test, higher zinc concentration of the Zn-HA increased the diameter of ZoI. Also with the addition of the citrate, the antibacterial effect was increased of Zn doped/undoped HA, as the diameters of the ZoI were larger than the non-citrate samples.

6 Future work

In the future, we will continue to study the antibacterial efficacy of this system. The release kinetics will also be studied by more release test.

For antibacterial study, streptomycin, a widely used antibiotic, will be incorporated into the Zn-citrate-HA system to test the bacterial killing efficiency. Further, to get the quantitative data, logarithm reduction test will be performed to give a quantitative result of antibacterial effect of this system.

References

1 Sader, H.S., Pignatari, A.C., Leme, I.L., Burattini, M.N., Tancresi, R., Hollis, R.J. and Jones, R.N. Epidemiologic Typing Of Multiply Drug-Resistant Pseudomonas-Aeruginosa Isolated From An Outbreak In An Intensive-Care Unit. *Diagnostic Microbiology and Infectious Disease*, 1993, **17**(1), 13-18.

2 Uhrich, K.E., Cannizzaro, S.M., Langer, R.S. and Shakesheff, K.M. Polymeric systems for controlled drug release. *Chemical Reviews*, 1999, **99**(11), 3181-3198.

3 Dasgupta, S., Banerjee, S.S., Bandyopadhyay, A. and Bose, S. Zn- and Mg-Doped Hydroxyapatite Nanoparticles for Controlled Release of Protein. *Langmuir*, 2010, **26**(7), 4958-4964.

4 Baker, S., Griffiths, C. and Nicklin, J. *BIOS Instatn Notes: Microbiology*. (Garland Science, 2011).

5 Lim, D.V. ***Microbiology***. (Kendall Hunt, 2002).

6 Nicklin, J., Graeme-Cook, K., Paget, T. and Killington, R.A. *Instant notes in microbiology*. (Springer, 1999).

7 Kumar, P.T.S., Abhilash, S., Manzoor, K., Nair, S.V., Tamura, H. and Jayakumar, R. Preparation and characterization of novel beta-chitin/nanosilver composite scaffolds for wound dressing applications. *Carbohydrate Polymers*, 2010, **80**(3), 761-767.

8 Darouiche, R.O. Current concepts - Treatment of infections associated with surgical implants. *New England Journal of Medicine*, 2004, **350**(14), 1422-1429.

9 Kerksiek, K. A life in slime – biofilms rule the world. (Infection Research: News and Pespective, 2008).

10 Khoo, X. and Grinstaff, M.W. Novel infection-resistant surface coatings: A bioengineering approach. *Mrs Bulletin*, 2011, **36**(5), 357-366.

11 Buckley, J.J., Lee, A.F., Olivi, L. and Wilson, K. Hydroxyapatite supported antibacterial Ag(3)PO(4) nanoparticles. *Journal of Materials Chemistry*, 2010, **20**(37), 8056-8063.

12 Montie, T.C. *Pseudomonas*. (Plenum Press, 1998).

13 Ramos, J.-L. ***Pseudomonas: Biosynthesis of macromolecules and molecular metabolism***. (Birkhäuser, 2004).

14 Rehm, B.H.A. Pseudomonas: Model Organism, Pathogen, Cell Factory. (Springer, 2010).

15 Cornelis, P. *Pseudomonas: genomics and molecular biology*. (Caister Academic Press, 2008).

16 Hirano, S.S. and Upper, C.D. POPULATION BIOLOGY AND EPIDEMIOLOGY OF PSEUDOMONAS-SYRINGAE. *Annual Review of Phytopathology*, 1990, **28**, 155-177.

17 Lindow, S.E. COMPETITIVE-EXCLUSION OF EPIPHYTIC BACTERIA BY ICE- PSEUDOMONAS-SYRINGAE MUTANTS. *Applied and Environmental Microbiology*, 1987, **53**(10), 2520-2527.

18 Vanneste, J.L. and Yu, J. Detection of *Pseudomonas Syringae* pv. *Papulans* in Apple Budwood. *New Zealand Plant Protection* 2006, **59**, *146-149*

19 Burr, T.J. and Hurwitz, B. Susceptibility of The Apple Cultivar Mutsu to Pseudomonas Syringae pv Papulans. *Phytopathology*, 1979, **69**(9), 1023-1023.
20 Evidente, A., Iacobellis, N.S., Impellizzeri, A. and Surico, G. Methyl (2,5-Dihydroxy-3-Nitrophenyl) Acetate from Pseudomonas syringae pv. papulans. *Phytochemistry*, 1992, **31**(12), 4105-4107.
21 Lee, J.H. Methicillin (oxacillin)-resistant Staphylococcus aureus strains isolated from major food animals and their potential transmission to humans. *Applied and Environmental Microbiology*, 2003, **69**(11), 6489-6494.
22 Baba, T., Takeuchi, F., Kuroda, M., Yuzawa, H., Aoki, K., Oguchi, A., Nagai, Y., Iwama, N., Asano, K., Naimi, T., Kuroda, H., Cui, L., Yamamoto, K. and Hiramatsu, K. Genome and virulence determinants of high virulence community-acquired MRSA. *Lancet*, 2002, **359**(9320), 1819-1827.
23 Langer, R. Drug delivery and targeting. *Nature*, 1998, **392**(6679), 5-10.
24 Vasir, J.K., Tambwekar, K. and Garg, S. Bioadhesive microspheres as a controlled drug delivery system. *International Journal of Pharmaceutics*, 2003, **255**(1-2), 13-32.
25 Muller, R.H., Jacobs, C. and Kayser, O. Nanosuspensions as particulate drug formulations in therapy Rationale for development and what we can expect for the future. *Advanced Drug Delivery Reviews*, 2001, **47**(1), 3-19.
26 Freiberg, S. and Zhu, X. Polymer microspheres for controlled drug release. *International Journal of Pharmaceutics*, 2004, **282**(1-2), 1-18.
27 Parfitt, A.M., Drezner, M.K., Glorieux, F.H., Kanis, J.A., Malluche, H., Meunier, P.J., Ott, S.M. and Recker, R.R. Bone Histomorphometry - standardization of nomenclature, symbols, and units. *Journal of Bone and Mineral Research*, 1987, **2**(6), 595-610.
28 Field, R.A., Riley, M.L., Mello, F.C., Corbridg.Mh and Kotula, A.W. Bone Composition In Cattle, Pigs, Sheep And Poultry. *Journal of Animal Science*, 1974, **39**(3), 493-499.
29 Legros, R., Balmain, N. and Bonel, G. Age-Related-Changes in Mineral of Rat and Bovine Cortical Bone. *Calcified Tissue International*, 1987, **41**(3), 137-144.
30 Brown, P.W. and Brent, C. *Hydroxyapatite and Related Materials*. (CRC Press Inc., 1994).
31 Kay, M.I., Young, R.A. and Posner, A.S. Crystal Structure of Hydroxyapatite. *Nature*, 1964, **204**(496), 1050-&.
32 Markovic, M., Fowler, B.O. and Tung, M.S. Preparation and comprehensive characterization of a calcium hydroxyapatite reference material. *Journal of Research of the National Institute of Standards and Technology*, 2004, **109**(6), 553-568.
33 Henkin, R.I., Lippoldt, R.E., Bilstad, J. and Edelhoch, H. Zinc Protein Isolated from Human Parotid Saliva. *Proceedings of the National Academy of Sciences of the United States of America*, 1975, **72**(2), 488-492.
34 Turgut, G., Abban, G., Turgut, S. and Take, G. Effect of overdose zinc on mouse testis and its relation with sperm count and motility. *Biological Trace Element Research*, 2003, **96**(1-3), 271-279.
35 Palazzo, B., Iafisco, M., Laforgia, M., Margiotta, N., Natile, G., Bianchi, C.L., Walsh, D., Mann, S. and Roveri, N. Biomimetic hydroxyapatite-drug nanocrystals as

potential bone substitutes with antitumor drug delivery properties. *Advanced Functional Materials*, 2007, **17**(13), 2180-2188.
36 Stanic, V., Dimitrijevic, S., Antic-Stankovic, J., Mitric, M., Jokic, B., Plecas, I.B. and Raicevic, S. Synthesis, characterization and antimicrobial activity of copper and zinc-doped hydroxyapatite nanopowders. *Applied Surface Science*, 2010, **256**(20), 6083-6089.
37 Santos, M.H., Valerio, P., Goes, A.M., Leite, M.F., Heneine, L.G.D. and Mansur, H.S. Biocompatibility evaluation of hydroxyapatite/collagen nanocomposites doped with Zn+2. *Biomedical Materials*, 2007, **2**(2), 135-141.
38 Ballo, A.M., Xia, W., Palmquist, A., Lindahl, C., Emanuelsson, L., Lausmaa, J., Engqvist, H. and Thomsen, P. Bone tissue reactions to biomimetic ion-substituted apatite surfaces on titanium implants (Journal of the Royal Society- Interface, 2012).
39 Otsuka, M., Marunaka, S., Matsuda, Y., Ito, A., Layrolle, P., Naito, H. and Ichinose, N. Calcium level-responsive in-vitro zinc release from zinc containing tricalcium phosphate (ZnTCP). *Journal of Biomedical Materials Research*, 2000, **52**(4), 819-824.
40 Bandyopadhyay, A., Bernard, S., Xue, W.C. and Bose, S. Calcium phosphate-based resorbable ceramics: Influence of MgO, ZnO, and SiO2 dopants. *Journal of the American Ceramic Society*, 2006, **89**(9), 2675-2688.
41 Commission, U.S.I.T. Citric Acid and Certain Citrate Salts from Canada and China, Invs. 701-TA-456 and 731-TA-1151-1152 (Preliminary). (DIANE Publishing, 2008).
42 Jiang, W.G., Pan, H.H., Cai, Y.R., Tao, J.H., Liu, P., Xu, X.R. and Tang, R.K. Atomic Force Microscopy Reveals Hydroxyapatite-Citrate Interfacial Structure at the Atomic Level. *Langmuir*, 2008, **24**(21), 12446-12451.
43 Leonards, J.R. and Free, A.H. The citrate content of the skeleton as influenced by prolonged feeding of acid-producing and base-producing salt. *Journal of Biological Chemistry*, 1944, **155**(2), 503-506.
44 Hu, Y.Y., Rawal, A. and Schmidt-Rohr, K. Strongly bound citrate stabilizes the apatite nanocrystals in bone. *Proceedings of the National Academy of Sciences of the United States of America*, 2010, **107**(52), 22425-22429.
45 Qiu, S.R., Wierzbicki, A., Salter, E.A., Zepeda, S., Orme, C.A., Hoyer, J.R., Nancollas, G.H., Cody, A.M. and De Yoreo, J.J. Modulation of calcium oxalate monohydrate crystallization by citrate through selective binding to atomic steps. *Journal of the American Chemical Society*, 2005, **127**(25), 9036-9044.
46 Sreenivasan, P.K., Furgang, D., Markowitz, K., McKiernan, M., Tischio-Bereski, D., Devizio, W. and Fine, D. Clinical anti-microbial efficacy of a new zinc citrate dentifrice. *Clinical Oral Investigations*, 2009, **13**(2), 195-202.
47 Balasundaram, G., Sato, M. and Webster, T.J. Using hydroxyapatite nanoparticles and decreased crystallinity to promote osteoblast adhesion similar to functionalizing with RGD. *Biomaterials*, 2006, **27**(14), 2798-2805.
48 Raynaud, S., Champion, E., Bernache-Assollant, D. and Thomas, P. Calcium phosphate apatites with variable Ca/P atomic ratio I. Synthesis, characterisation and thermal stability of powders. *Biomaterials*, 2002, **23**(4), 1065-1072.

49 Kumar, R., Prakash, K.H., Cheang, P. and Khor, K.A. Temperature driven morphological changes of chemically precipitated hydroxyapatite nanoparticles. *Langmuir*, 2004, **20**(13), 5196-5200.
50 Chai, C.S. and Ben-Nissan, B. Bioactive nanocrystalline sol-gel hydroxyapatite coatings. *Journal of Materials Science-Materials in Medicine*, 1999, **10**(8), 465-469.
51 Bouyer, E., Gitzhofer, F. and Boulos, M.I. Morphological study of hydroxyapatite nanocrystal suspension. *Journal of Materials Science-Materials in Medicine*, 2000, **11**(8), 523-531.
52 Afshar, A., Ghorbani, M., Ehsani, N., Saeri, M.R. and Sorrell, C.C. Some important factors in the wet precipitation process of hydroxyapatite. *Materials & Design*, 2003, **24**(3), 197-202.
53 Leeuwenburgh, S.C.G., Ana, I.D. and Jansen, J.A. Sodium citrate as an effective dispersant for the synthesis of inorganic-organic composites with a nanodispersed mineral phase. *Acta Biomaterialia*, 2010, **6**(3), 836-844.
54 Sambrook, J., Fritsch,EF, Maniatis,T. *Molecular Cloning: A Laboratory Manual*. (Cold Spring Harbor Press, 1989).
55 Meng, Y.Z., Qin, Y.X., DiMasi, E., Ba, X.L., Rafailovich, M. and Pernodet, N. Biomineralization of a Self-Assembled Extracellular Matrix for Bone Tissue Engineering. *Tissue Engineering Part A*, 2009, **15**(2), 355-366.
56 Abdi, K., Nafisi, S., Manouchehri, F., Bonsaii, M. and Khalaj, A. Interaction of 5-Fluorouracil and its derivatives with bovine serum albumin. *Journal of Photochemistry and Photobiology B-Biology*, 2012, **107**, 20-26.